

 Open access • Journal Article • DOI:10.1016/S0168-9002(02)00800-8

## Particle identification method in the CsI(Tl) scintillator used for the CHIMERA 4 $\pi$ detector — Source link

Monica Alderighi, A. Anzalone, R Bassini, I. Berceanu ...+58 more authors

**Institutions:** University of Silesia in Katowice, University of Paris-Sud, University of Caen Lower Normandy, University of Bologna ...+4 more institutions

**Published on:** 21 Aug 2002 - Nuclear Instruments & Methods in Physics Research Section A-accelerators Spectrometers Detectors and Associated Equipment (North-Holland)

**Topics:** Particle identification, Scintillator, Charged particle and Hermetic detector

Related papers:

- [Fragmentation studies with the CHIMERA detector at LNS in Catania: recent progress](#)
- [Mass and charge identification of fragments detected with the Chimera Silicon–CsI\(Tl\) telescopes](#)
- [Isospin dependence of incomplete fusion reactions at 25 MeV/nucleon.](#)
- [Constrained molecular dynamics approach to fermionic systems](#)
- [Studies of Nuclear Reactions and Time Scale with the 4 \$\pi\$  Detector CHIMERA](#)

Share this paper:    

View more about this paper here: <https://typeset.io/papers/particle-identification-method-in-the-csi-tl-scintillator-1m3znhzolt>



## Particle identification method in the CsI(Tl) scintillator used for the CHIMERA $4\pi$ detector

M. Alderighi<sup>a</sup>, A. Anzalone<sup>b</sup>, R. Bassini<sup>c</sup>, I. Berceanu<sup>d</sup>, J. Blicharska<sup>e</sup>, C. Boiano<sup>c</sup>, B. Borderie<sup>f</sup>, R. Bougault<sup>g</sup>, M. Bruno<sup>h</sup>, C. Cali<sup>b</sup>, G. Cardella<sup>i,\*</sup>, Sl. Cavallaro<sup>b,j</sup>, M. D'Agostino<sup>h</sup>, M. D'Andrea<sup>i</sup>, R. Dayras<sup>k</sup>, E. De Filippo<sup>i</sup>, F. Fichera<sup>i</sup>, E. Geraci<sup>b,j</sup>, F. Giustolisi<sup>b,j</sup>, A. Grzeszczuk<sup>e</sup>, N. Guardone<sup>i,j</sup>, P. Guazzoni<sup>c</sup>, D. Guinet<sup>l</sup>, C.M. Iacono-Manno<sup>b,j</sup>, S. Kowalski<sup>e</sup>, E. La Guidara<sup>b,j</sup>, A.L. Lanchais<sup>h</sup>, G. Lanzalone<sup>b,j</sup>, G. Lanzano<sup>i</sup>, N. Le Neindre<sup>h,g</sup>, S. Li<sup>m</sup>, C. Maiolino<sup>b</sup>, Z. Majka<sup>n</sup>, G. Manfredi<sup>c</sup>, D. Nicotra<sup>i</sup>, T. Paduszynski<sup>e</sup>, A. Pagano<sup>i</sup>, M. Papa<sup>i</sup>, C.M. Petrovici<sup>d</sup>, E. Piasecki<sup>o</sup>, S. Pirrone<sup>i</sup>, G. Politi<sup>i,j</sup>, A. Pop<sup>d</sup>, F. Porto<sup>b,j</sup>, M.F. Rivet<sup>f</sup>, E. Rosato<sup>q</sup>, G. Saccá<sup>i</sup>, G. Sechi<sup>a</sup>, V. Simion<sup>d</sup>, M.L. Sperduto<sup>b,j</sup>, J.C. Steckmeyer<sup>g</sup>, A. Trifiró<sup>p</sup>, M. Trimarchi<sup>p</sup>, S. Urso<sup>i</sup>, G. Vannini<sup>h</sup>, M. Vigilante<sup>q</sup>, J. Wilczynski<sup>r</sup>, H. Wu<sup>m</sup>, Z. Xiao<sup>m</sup>, L. Zetta<sup>c</sup>, W. Zipper<sup>e</sup>

<sup>a</sup>INFN sez. Milano and Istituto di Fisica Cosmica CNR, Milano, Italy

<sup>b</sup>INFN, Laboratorio Nazionale del Sud, Catania, Italy

<sup>c</sup>Dip. di Fisica dell'Università and INFN sez. di Milano, Milano, Italy

<sup>d</sup>Institute for Physics and Nuclear Engineering, Bucharest, Romania

<sup>e</sup>Institute of Physics, University of Silesia, 40-007 Katowice, Poland

<sup>f</sup>IPN, IN2P3-CNRS and Université Paris-Sud, Orsay, France

<sup>g</sup>LPC, ISMRA Université de Caen, France

<sup>h</sup>INFN, Sezione di Bologna and Dip. di Fisica Università di Bologna, Italy

<sup>i</sup>Laboratori Nazionali del Sud, INFN, Sezione di Catania, Via S. Sofia 44, I-95123 Catania, Italy

<sup>j</sup>Dip. di Fisica e astronomia dell'Università di Catania, Catania, Italy

<sup>k</sup>DAPNIA-SPhN, CEA Saclay, France

<sup>l</sup>IPN, IN2P3-CNRS and Université Claude Bernard, Lyon, France

<sup>m</sup>Institute of Modern Physics, Chinese Academy of Sciences, China

<sup>n</sup>Institute of Physics, Jagellonian University, Krakow, Poland

<sup>o</sup>Inst. of Exper. Physics, University of Warsaw, Poland

<sup>p</sup>INFN and Dipartimento di Fisica Università di Messina, Italy

<sup>q</sup>Dip. di Scienze Fisiche dell'Università "Federico II" and INFN sez. di Napoli, 80126 Napoli, Italy

<sup>r</sup>Institute for Nuclear Studies Otwock-Swierk, Poland

Received 7 December 2001; received in revised form 13 February 2002; accepted 13 February 2002

\*Corresponding author.

E-mail address: cardella@ct.infn.it (G. Cardella).

## Abstract

The charged particle identification obtained by the analysis of signals coming from the CsI(Tl) detectors of the CHIMERA  $4\pi$  heavy-ion detector is presented. A simple double-gate integration method, with the use of the cyclotron radiofrequency as reference time, results in low thresholds for isotopic particle identification. The dependence of the identification quality on the gate generation timing is discussed. Isotopic identification of light ions up to Beryllium is clearly seen. For the first time also the identification of  $Z = 5$  particles is observed. The identification of neutrons interacting with CsI(Tl) by  $(n, \alpha)$  and  $(n, \gamma)$  reactions is also discussed. © 2002 Elsevier Science B.V. All rights reserved.

PACS: 29.40.-n; 29.40.Wk

Keywords: CsI(Tl) detectors; Pulse-shape method; Time of flight; Particle identification method

## 1. Introduction

Experiments aimed to investigate phase transitions and effects associated with the isospin degree of freedom in heavy-ion induced multi-fragmentation reactions were recently undertaken at Laboratori Nazionali del Sud (LNS) in Catania by using the forward part (from  $\theta = 1^\circ$  to  $30^\circ$ ) of the CHIMERA detector [1]. High-quality beams of  $^{124}\text{Sn}$  and  $^{112}\text{Sn}$  at 35 MeV/A with an intensity of about  $5 \times 10^7$  particles/s were delivered by the super-conducting cyclotron to bombard  $^{27}\text{Al}$ ,  $^{58}\text{Ni}$  and  $^{64}\text{Ni}$  thin ( $200 \mu\text{g}/\text{cm}^2$ ) targets [2]. The experimental setup consists of 688 Silicon–CsI telescopes representing the forward part of the complete detection system made of 1192 telescopes. Detectors were mounted in 9 rings centered along the beam axis at a distance ranging from 1 to 3.5 m from the target. CsI(Tl) scintillators, placed in the telescopes behind silicon detectors, give the residual energy of detected heavy ions, and in case of light particles, enable identification of their charge and mass. In order to avoid temperature instability in the electronics under vacuum and the well-known effect of the temperature dependence of the CsI(Tl) response function [3], a remote controlled cooling system is used. A photodiode readout of CsI(Tl) has been chosen because large area photodiodes ( $18 \times 18 \text{ mm}^2$ ) were less expensive than photomultipliers. Their stability has been extensively checked and proved. Besides, the use of photodiodes does not affect the particle identification performance of CsI(Tl) detectors, as reported in

many experimental works [4–11]. In particular, as shown in Ref. [12], a good identification has been achieved with some prototypes of our rather large crystals, which in the forward region have typical size  $5 \times 5 \times 12 \text{ cm}^3$ . In that work we emphasized the importance of having crystals of good uniformity. All the CHIMERA CsI(Tl) crystals were therefore selected in order to show a uniform response to  $\alpha$ -particles and  $\gamma$ -rays irradiation. Obviously, the uniformity request is also essential for obtaining a good energy resolution. (See recently published Ref. [13].) In this paper the obtained results and solutions improving the particle discrimination, achieved earlier [12] for a few crystals, are discussed. This work extends the identification method to the complete CHIMERA  $4\pi$  detector. After this introduction including a short description of the detector, in Section 2 the identification methods used for CsI(Tl) detectors are reminded and the obtained results are presented. In Section 3 the advantages of the used method are discussed. In Section 4 some possible extension of the method to neutron detection and the conclusive remarks are presented.

## 2. The particle identification method and results

Particle identification using the photodiode signal of CsI(Tl) detectors can be obtained in different ways: a standard pulse shape method, similar to the one used for neutron- $\gamma$  discrimination, has been used in Ref. [4–6,8,11]; a two-gate method [7,9,12], with a simpler electronics or a

combination of the two methods [10], have shown also rather good results. Very recently, a digital signal analysis has also been carried out and reported in Ref. [14].

The two-gate method, applied to a photodiode with charge preamplifier readout, is based on the fact that the decay time of the unipolar signal of a spectroscopic amplifier (under proper shaping time conditions) keeps memory of the mass and charge of the detected particles. By integrating a portion of the tail of the amplifier output and plotting this value (SLOW-component) against a signal proportional to the peak value (FAST-component) giving the energy information), the identification scatter plot shown in Fig. 1 was produced. This picture, obtained in the reaction  $^{124}\text{Sn} + ^{64}\text{Ni}$  at 35 MeV/A for one of the CHIMERA detectors, mounted at  $\theta = 14^\circ$ , illustrates typical features of the identification function in the experiment. Spectroscopy amplifier, 16-channel Silena 761F

with  $2\ \mu\text{s}$  shaping time were used. As can be observed, a satisfactory particle identification is obtained. The mass separation is better seen in the insets in Fig. 1, where  $^{7,9}\text{Be}$  isotopes are clearly observed, and even boron ions can be discriminated from heavier ions, achievements reached to our knowledge for the first time in application of this method. The isotopic identification has been verified using the information on the energy loss in the preceding silicon detector. In the next section will be shown that the quality of the obtained identification depends on the time stability reached with our gate generation method.

### 3. The gate generation method

For the charge integration, 9U QDC manufactured by CAEN (mod. VN1465) were used. Such

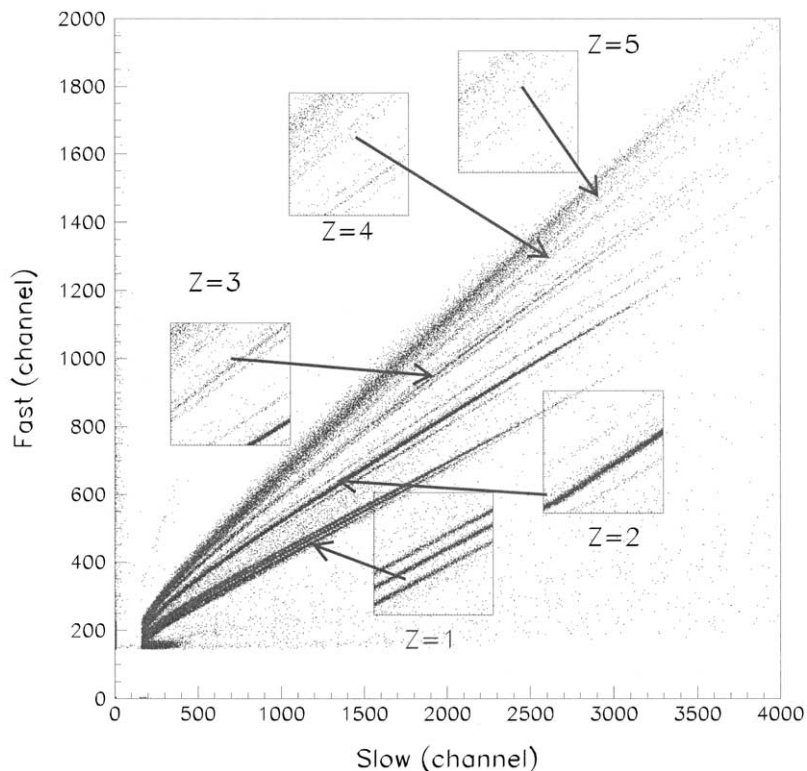


Fig. 1. FAST–SLOW identification scatter plot obtained for one of the 688 crystals located at  $\theta = 14^\circ$  relative to the beam direction in the  $^{124}\text{Sn} + ^{64}\text{Ni}$  reaction. The insets show expanded portions of the scatter plot.

QDC have a common gate and, for simplicity, the same gate for all the 688 telescopes was used.

The CHIMERA detector is designed to provide mass identification of particles by measuring their time of flight (TOF). Therefore, detectors are mounted at large distances from the target up to 3.5 m for the very forward angles. The long fly paths ensure the time spread necessary for mass identification, but on the other hand, they result in a time jitter of the signals with respect to the used common gate. To overcome this problem, in analysing the FAST-component, high-quality low-cost 48-channel stretcher modules designed by INFN Milano, are used. In this way, the energy resolution of the CsI(Tl) detectors is not affected by any dynamical jitter.

The SLOW gate (as well as the others) is generated using as reference time the radiofrequency (RF) of the cyclotron accelerator validated by the trigger, see Fig. 2. As a consequence of using the RF reference time, coincidences with particles produced within different beam bursts (spurious events, dashed signal of Fig. 2) are characterized by a SLOW integrated signal quite different than the one collected for good coincidences. These spurious events are seen in Fig. 1 as random noise because at the measured angle ( $\theta = 14^\circ$ ) the rate of spurious coincidences was small (around 0.8%, in agreement with the trigger rate and the average single rate in the detector). On the contrary, particles produced in different beam bursts are clearly seen in Fig. 3 showing data from a detector of the first ring, mounted at  $\theta = 1^\circ$ . At such a small angle, due to the high rate of elastic scattered particles (1 kHz for an individual detector), there is a higher probability to observe spurious coincidences (of the order of 4%). Fig. 3 shows that due to the presence of the stretcher, the FAST signal is independent on the beam burst while the SLOW-component is sampled (look also at the gate timing sketched in Fig. 2) in a wide range of the signal height. By fitting the observed distribution of the events corresponding to spurious coincidences with different beam bursts in Fig. 3, one can determine the dependence of the SLOW-component on the time jitter of the signal. One obtains a 6% variation of the SLOW-component signal (pedestal subtracted)

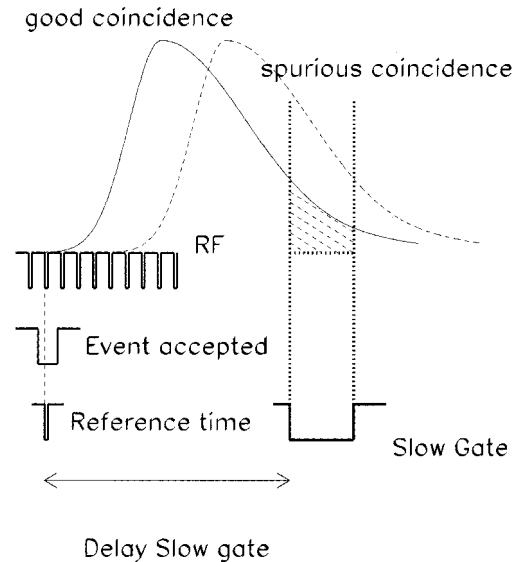


Fig. 2. Sketch of the slow gate timing. The “event accepted” signal, produced by the trigger, enables one RF signal. This signal is used as reference time to generate all gates. The dashed region shows the SLOW integration region of a signal produced by a good coincidence. One can note the difference with the charge integrated with the same gate for a signal produced in a different burst (dashed signal spurious coincidence). The time scale of the real experiment has been not respected to better evidence the effect.

each 134 ns, being this value the time difference between two consecutive beam bursts. This information was used to study the effect of the signal jitter on particle identification resolution. In Fig. 4 a typical energy-SLOW scatter plot, expanded in the low-energy region is shown. No pedestal suppression in the SLOW-component signal was done for this detector, allowing to observe the low-energy region without threshold. The CsI energy is obtained calibrating the FAST-component with protons of known energy. A first calibration point was obtained using a 26.1 MeV proton beam. At low-energy other calibration points were obtained using the protons observed in the  $\Delta E-E$  scatter plots. The energy that such protons release in the CsI(Tl) detectors ranges from 2 to 6 MeV and was determined using an independent calibration of the  $\Delta E$  silicon detectors and energy loss calculations. It can be seen that above 20 MeV, one can easily

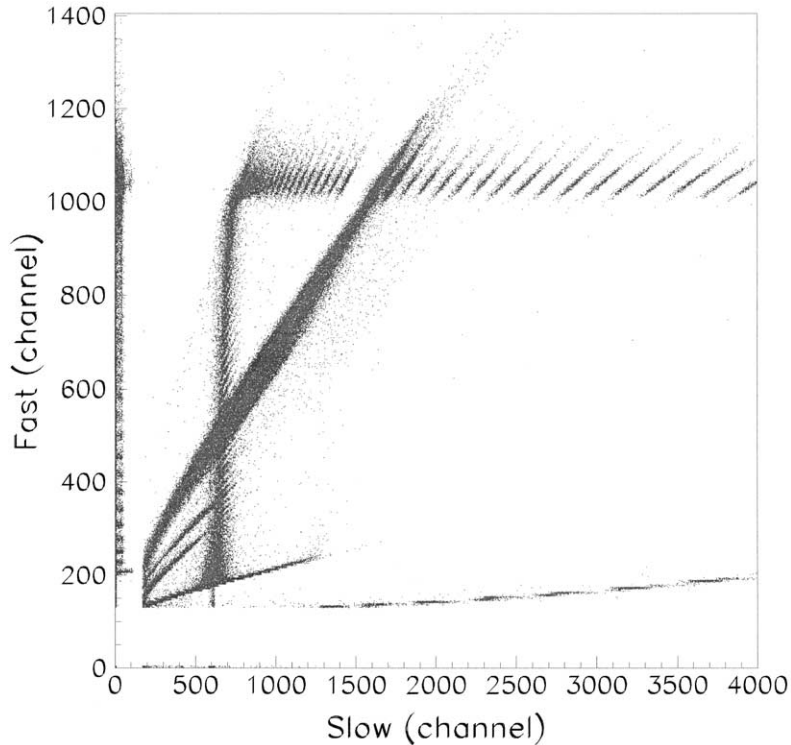


Fig. 3. FAST–SLOW identification scatter plot for a detector located at  $\theta = 1^\circ$ . The observed lines with constant value of the FAST-component are due to spurious coincidences in different beam bursts. As can be seen in Fig. 2 the variation in the SLOW signal is due to the dependence of the position of the SLOW gate on the RF signal.

distinguish tritons (t) from deuterons (d) (look also to the upper inset of Fig. 4 where a plot of the SLOW/FAST signal obtained for a slice around 20 MeV protons is shown). The distance along the SLOW axis between d and t lines at 20 MeV is of the order of 100 channels. With the time dependence of the SLOW signal determined as described above, one obtains the dispersion of about 0.5 ch/ns. The very low RF time spread, 700–800 ps (FWHM) measured during the run, is therefore negligible. Furthermore, the dependence of the SLOW-component upon the particle velocity is also small. For example, the TOF difference between 20 MeV deuterons and tritons detected at a distance of 1.6 m (for data presented in Fig. 3) is 8 ns. As the deuterons are faster than tritons for a fixed kinetic energy, their signal is produced earlier in the CsI(Tl) detector and therefore, the

SLOW gate will start 8 ns later respect to it. For the estimated dispersion of the SLOW-component of 0.5 ch/ns, this will result in a very small reduction (4 channels) of the distance between the deuteron and triton lines. This value approximately doubles for detectors of the first ring, placed at the distance of 3.5 m; nevertheless, it remains small when compared with the distance between the two lines. These first-order estimates should be further corrected by accounting for the quenching effect and the difference in energy loss in silicon detector in front of the CsI(Tl) detector. Both effects require a correction increasing the energy of tritons that would be necessary to produce the same light signal as that for deuterons of the same energy. This correction decreases the estimated time difference for the two considered particles.

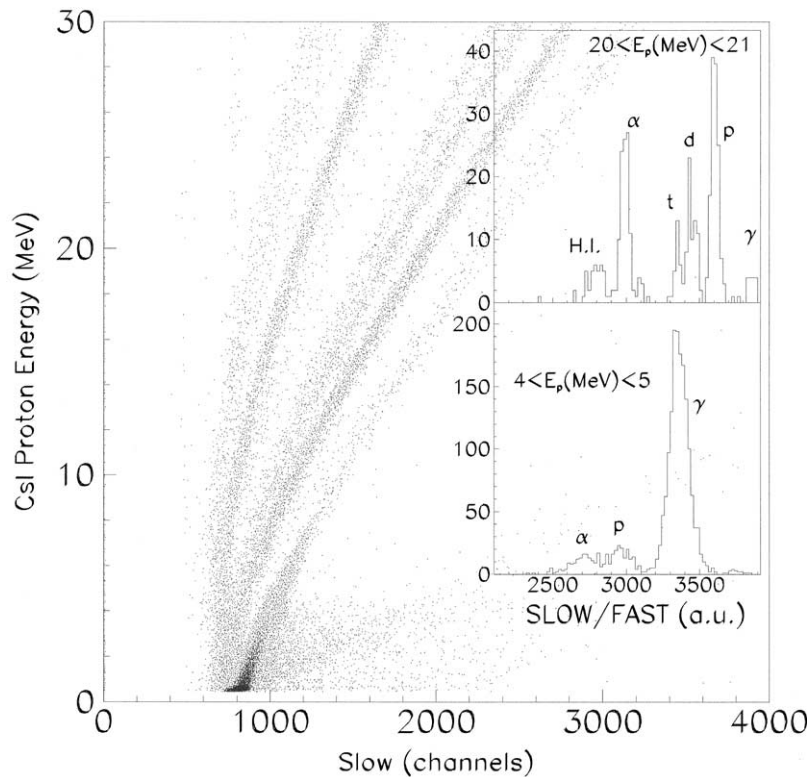


Fig. 4. Energy-SLOW component scatter plot. The energy is obtained calibrating the FAST-component with protons of known energy. This permits to evaluate the energy threshold for particle identification. To better evaluate the quality of the isotopic identification, in the insets are plotted linearized (SLOW/FAST) projections of slices of this scatter plot.

In comparison with the previous CHIMERA collaboration work [12], in which the gates were generated by the time signal from the CsI(Tl), the main advantage obtained using the RF signal as time reference is a significant reduction of the identification thresholds. With the previous method [12], the charge identification threshold for proton and alpha particles was above 8 MeV, whereas in the present work a typical threshold for protons about 4–5 MeV is obtained, as can be seen from Fig. 4 looking also to the lower inset. The identification threshold for discrimination of charged particles against  $\gamma$ -rays is  $<2$  MeV (proton energy). Taking into account the large size of crystals used in CHIMERA, our results obtained in normal on-beam conditions are rather good in comparison with the best results reported in the

literature [9,14]. We remind that the low thresholds reported in these works [9,14] were achieved, in fact, for small crystals irradiated with radioactive sources [9,14]. Our old results are typical for rather poor time stability [6] that can be obtained by triggering the gate with a standard discriminator acting on the CsI(Tl) signal coupled with photodiode.

#### 4. The neutron identification and final remarks

Effects of an influence of the TOF on the FAST-SLOW identification scatter plots have interesting consequences allowing one to observe signals produced by neutrons interacting with CsI(Tl) detectors. In the inset of Fig. 1 for

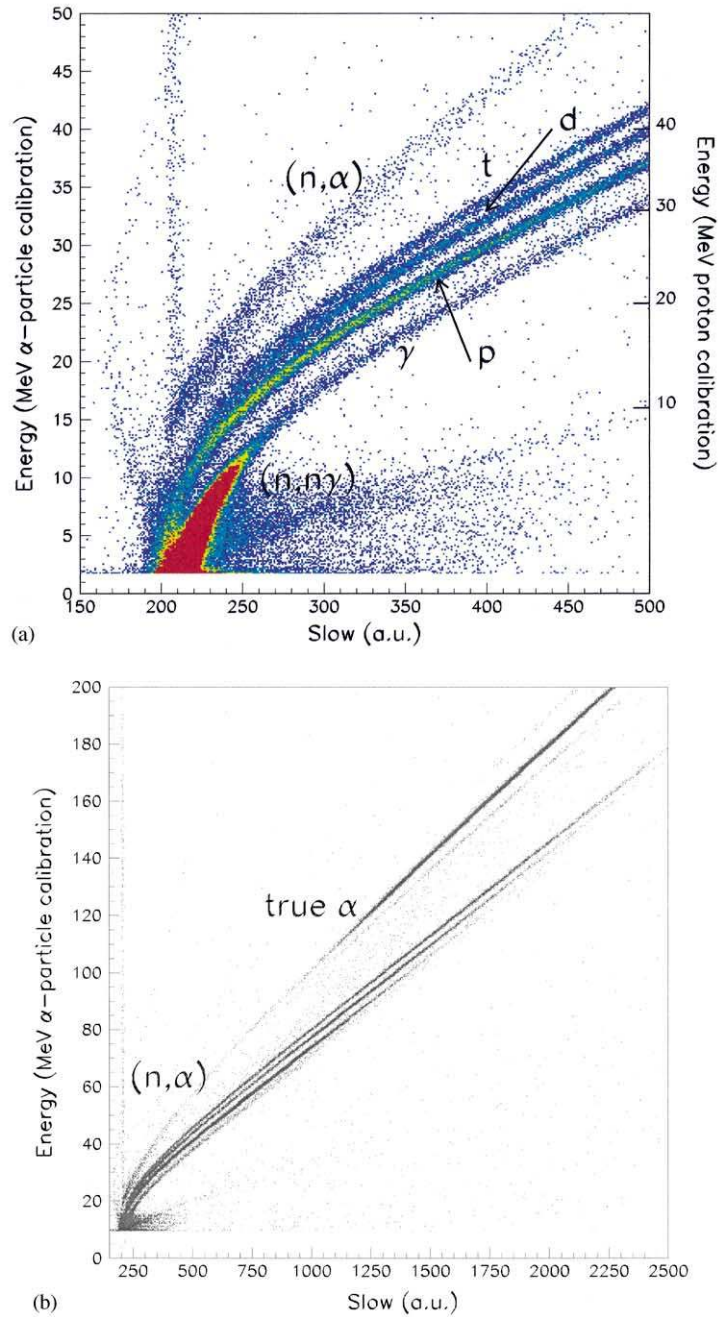


Fig. 5. (a) Low-energy zoom of an energy-SLOW scatter plot calibrated in  $\alpha$ -particle (left scale) and proton equivalent energy (right scale) for the same detector as in Fig. 4. Only particles that do not produce signals in the silicon detector in front of the CsI(Tl) crystal are plotted. Thus  $\alpha$ -particles originating from  $(n, \alpha)$  reactions are observed. Protons, deuterons and tritons that do not release enough energy in the silicon detector to overcome the QDC threshold are also observed. (b) Same scatter plot as (a) but without zoom,  $\alpha$ -particles of energy higher than 100 MeV that do not release enough energy in the silicon detector can be observed.



$Z = 2$ , a shadow near the alpha line can be seen. This shadow is produced by neutrons interacting with the CsI(Tl) detector through  $(n, \alpha)$  reactions. The TOF of an  $\alpha$ -particle generated by the  $(n, \alpha)$  reaction corresponds to the velocity of the primary neutron. Therefore, for  $\alpha$ -particles produced in the target or via  $(n, \alpha)$  reactions the TOF differs by more than a factor of two. This produces a large time spread and thus the shadow observed in Fig. 1. To confirm this hypothesis, we have additionally used information from the silicon detector. Obviously,  $\alpha$ -particles must give a signal also in the silicon detector placed in front of the CsI(Tl), whereas neutrons do not (the interaction probability of neutrons with the 300  $\mu\text{m}$  silicon detector is negligible respect to the interaction probability with the 12 cm long CsI(Tl) scintillator). In Fig. 5a is presented a zoom of the low-energy region of a energy-SLOW scatter plot obtained with the condition of no signal in the silicon detector. One can see the  $(n, \alpha)$  line starting from about 14 MeV in the  $\alpha$ -particle calibration scale. This is in good agreement with the expected threshold for the  $(n, \alpha)$  process ( $\alpha$  energy calibration of the fast component was obtained using points from the  $\Delta E(\text{silicon})-E(\text{FAST CsI(Tl)})$  scatter plot using energy loss calculations and the silicon detector calibration). In Fig. 5a apart from  $(n, \alpha)$  and  $\gamma$  lines one can see also p, d and t lines. They originate from particles that do not release enough energy in the silicon detector to be seen by the QDC. As a matter of fact, high-energy  $^3\text{He}$  and  $\alpha$ -particles produced in the target may also generate a too small signal in the silicon. Their presence can be observed at higher energy,  $E_\alpha > 100$  MeV in Fig. 5b, that show without zoom all collected data. There is one more effect in Fig. 5a that we would like to comment: one can observe a concentration of events to the right of the  $\gamma$  line. These events can be produced by low-energy neutrons interacting with the detector through  $(n, \gamma)$  reactions. The TOF delay for low-energy neutrons of a few MeV, relative to  $\gamma$ -rays on the 1.6 m flight path, is of the order of 100 ns. The signal is delayed with respect to the SLOW gate and therefore more charge is integrated producing a larger SLOW signal for the same light output.

Additional simulations and tests are necessary to confirm this hypothesis.

In summary, we have shown that a satisfactory identification of light particles can be obtained in a large array of CsI(Tl) detectors with photodiode readout and a compact cheap electronics when a stable reference time is used to generate the gates for the QDC analysis. Although in our work a particularly good reference time ( $\leq 1$  ns) was used, our method could be effectively applied even with somewhat worst time resolution, probably up to 4–5 ns. Using this method combining the pulse shape identification and the TOF information, for the first time particles up to  $Z = 5$  are identified whereas isotopic identification is attained up to  $Z = 4$ . The TOF influence on this particle identification method could be also fundamental to discriminate neutron from  $\gamma$ -rays.

### Acknowledgements

The LNS cyclotron staff is greatly acknowledged for producing beams of very high quality. We would like also to thank all the technical staffs of the INFN Sezione di Catania and LNS for the enthusiastic effort that led to successful mounting of the CHIMERA detector.

### References

- [1] S. Aiello, et al., Nucl. Phys. A 583 (1995) 461c.
- [2] A. Pagano, et al., Nucl. Phys. A 681 (2001) 33.
- [3] J. Valentine, W. Moses, S. Derenzo, D. Wehe, G. Knoll, Nucl. Instr. and Meth. A 325 (1993) 147; J. Valentine, D. Wehe, G. Knoll, C. Moss, IEEE Trans. Nucl. Sci. 40 (1993) 1267 (see also Refs. [4–7]).
- [4] P. Kreutz, A. Kühmichel, C. Pinkenburg, J. Pochodzalla, Z.Y. Guo, U. Lynen, H. Sann, W. Trautmann, R. Trockel, Nucl. Instr. and Meth. A 260 (1987) 120.
- [5] R.J. Meijer, G.I. Van Nieuwenhuizen, A. Van Den Brink, P. Decowski, K.A. Griffioen, R. Kamermans, Nucl. Instr. and Meth. A 264 (1988) 285.
- [6] W.G. Gong, et al., Nucl. Instr. and Meth. A 268 (1988) 190.
- [7] D. Guinet, et al., Nucl. Instr. and Meth. A 278 (1989) 614.

- [8] X. Hongfei, Z. Wenlong, G. Zhongyan Zhu Yongtai, Z. Jianqun, W. Jinchuan, L. Guanhua Fan Enjie, *Nucl. Instr. and Meth. A* 320 (1992) 504.
- [9] M. Moszyński, D. Wolski, T. Ludziejewski, S.E. Arnell, Ö. Skeppstedt, W. Klamra, *Nucl. Instr. and Meth. A* 336 (1993) 587.
- [10] D.G. Sarantites, P.F. Hua, M. Devlin, L.G. Sobotka, J. Elson, J.T. Hood, D.R. LaFosse, J.E. Sarantites, M.R. Maier, *Nucl. Instr. and Meth. A* 381 (1996) 418.
- [11] R. Laforest, E. Ramakrishnan, D.J. Rowland, R. Delafield, S. Guzman, S. Ferro, S. Vasal, E. Winchester, S.J. Yennello, *Nucl. Instr. and Meth. A* 404 (1998) 470.
- [12] S. Aiello, et al., *Nucl. Instr. and Meth. A* 369 (1996) 50.
- [13] A. Wagner, et al., *Nucl. Instr. and Meth. A* 456 (2001) 290.
- [14] W. Skulski, M. Momayezi, *Nucl. Instr. and Meth. A* 458 (2001) 759.